J. Phys. Chem. A **2000,** *104,* 9675−9680

Gas-Phase Photoemission Study of 2-Mercaptobenzoxazole

G. Contini*

C.N.R., Institute of Mineral Processing, Via Bolognola 7, 00138 Rome, Italy

V. Di Castro

Dipartimento di Chimica, Università di Roma "La Sapienza", P.le A. Moro 5, 00185 Rome, Italy

S. Stranges

Dipartimento di Chimica, Università di Roma "La Sapienza" ed Unità INFM, P.le A. Moro 5, 00185 Rome, Italy

R. Richter

Sincrotrone Trieste, 34012 Basovizza, Trieste, Italy

M. Alagia

TASC-INFM, Area Science Park, 34012 Basovizza, Trieste, Italy

Received: May 31, 2000; In Final Form: August 7, 2000

The valence electronic structure of 2-mercaptobenzoxazole has been studied experimentally by synchrotron radiation photoelectron spectroscopy (PES) in the gas phase, and theoretically at ab initio level. The comparison of experiment and theory shows that only one of the two tautomers of 2-mercaptobenzoxazole, the thione form, is present in the vapor phase. The equilibrium molecular geometry for both forms has been obtained at MP2 level, and the results show that the thione tautomer is the most stable one. Despite the large size of the molecule, vibrational structure has been clearly observed in the photoelectron spectrum for the lowest three electronic states. Carbon 1s and sulfur 2p photoelectron spectra of 2-mercaptobenzoxazole vapor have also been investigated. The experimental ionization potential values of the seven chemically different carbon atoms have been obtained and found in good agreement with the results of ab initio calculations. High-resolution total-ion-yield spectra have been recorded in the gas phase near the carbon K-edge and sulfur $L_{2,3}$-edges. Experimental features due to the resonant decay of core-excited states have been observed and compared with the corresponding near-edge X-ray-absorption fine structure (NEXAFS) spectra of multilayer 2-mercaptobenzoxazole. The experimental spectra have been also compared with theoretical NEXAFS spectra of the free molecule calculated by the ab initio STEX method. Differences between the gas-phase and the multilayer 2-mercaptobenzoxazole have been observed and are discussed.

Introduction

The study of heterocyclic molecules and their adsorption on metals is of considerable importance both from a theoretical and a technological point of view. In recent years various surface investigations have been devoted to the study of the adsorption on metals of molecules with an aromatic ring and a heteroatomic part.[1−9] These molecules are interesting because of their applications as corrosion inhibitors, flotation collectors, and for their ability to form self-assembled layers. The main technological application of 2-mercaptobenzoxazole (C_7H_5NOS, in the following MBO) is in flotation processes because it belongs to a class of particularly active chelating agents.[10] The knowledge of the electronic structure of the free molecule is valuable information to better understand the interaction and bond formation between the chelating molecule and the surface.

Molecules that are solids at room temperature and pressure, such as MBO, can be vaporized in vacuum onto a surface to form adsorbed layers. In such experiments, photoemission can give information on the molecule/surface and intermolecular interactions. Obviously, it is crucially important to identify and study the species in the vapor phase, this being the entity interacting with the surrounding environment. Moreover, in the case of MBO two tautomeric forms may exist in the high-temperature vapor: the thione (NH) and the thiol (SH) forms, the first with a C=S double bond, the latter having the endocyclic double bond C=N and the hydrogen atom bonded to the sulfur atom instead of the nitrogen (see Figure 1). The valence electronic structure of the free molecule is sensitive to the difference in chemical structure and allows the two tautomers to be distinguished.

In this paper we report results of the first gas-phase photoemission investigation of MBO vapor. Valence photoelectron (PE) spectra obtained at different photon energies are shown

---

* Corresponding author. Fax: +39-068804463. E-mail: continig@iasi.rm.cnr.it.

10.1021/jp001979d CCC: $19.00

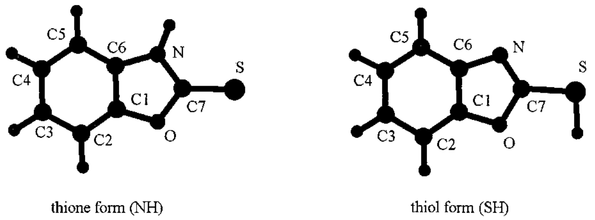

thione form (NH) thiol form (SH)

Figure 1. 2-Mercaptobenzoxazole (MBO) tautomers: thione form (NH) (left) and thiol form (SH) (right). The numbering of the seven carbon atoms is used in text.

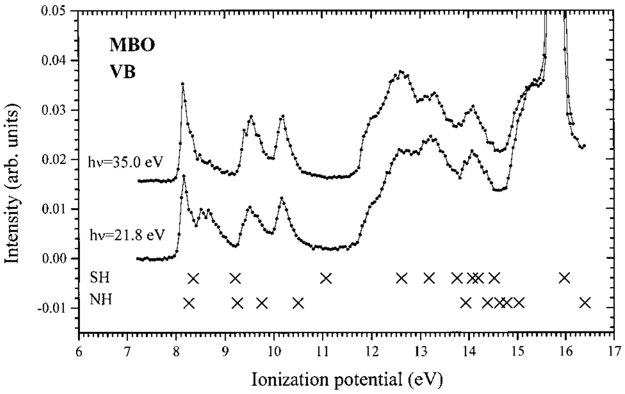

Figure 2. Valence PE spectrum of MBO vapor obtained at 21.8 and 35.0 eV photon energy. The argon photoionization line at 15.76 eV is used for energy calibration. The calculated orbital energies for the outermost MOs of both thione (NH) and thiol (SH) tautomers are reported in the bottom part as crosses.

and the assignment of the observed features is given based on ab initio calculations. C 1s and S 2p PE spectra are presented together with total-ion-yield spectra (near-edge X-ray absorption fine structure, NEXAFS) recorded in the respective edge regions.

Experimental Section

The experiment has been carried out using the ARPES end-station of the Gas-Phase beamline at Elettra. Details of the beamline and the experimental station have been given elsewhere,[11] so only the major features relevant to the present experiment will be described here. Photoelectron spectra have been recorded using a hemispherical photoelectron energy analyzer (VSW, 50 mm mean radius). The analyzer was operated in the constant pass energy mode. Pass energies of 5, 10, and 25 eV were used in the course of this experiment. The total-ion-yield spectra were recorded using a time-of-flight spectrometer, collecting all ions arriving at the detector. At the initial stages of the experiment mass spectra were also recorded at 21.22 eV photon energy (HeI line). In those spectra no ions with masses higher than the molecular peak were detected.

The position of the spectrometers with respect to the polarization vector of the synchrotron radiation could be rotated under vacuum and was kept at the "magic angle" (54.7°) throughout the PE experiments. The total-ion-yield spectra were collected in the direction of the light polarization vector. The photon energy calibration of the two gratings used in the sulfur $L_{2,3}$-edge and carbon K-edge regions is based on the Kr $3d_{5/2} \rightarrow 6p$ and $3d_{5/2} \rightarrow 5p$ resonance lines (valley at 92.51 eV[12]), the Ar $4s \rightarrow 2p_{3/2}$ resonance feature recorded in second diffraction order (122.19 eV[13]), the SF_6 absorption peak at 178.63 eV,[14] the N_2 $1s \rightarrow \pi^*$ vibronic resonances (second- and first-order lines at 200.55 and 401.10 eV, respectively[13]), and the Ar $2p_{3/2} \rightarrow 4s$ resonance at 244.37 eV[13] using the first-order monochromator scan. During the experiment the photon energy calibration was checked recording total-ion-yield spectra of Ar in the $2p_{3/2} \rightarrow 4s$ excitation region in a gas cell located behind the experimental chamber using first- and second-order monochromator scans. The kinetic energy scale of the analyzer was calibrated by introducing suitable gases (Ar, SF_6) into the ionization region together with the sample and recording a photoelectron spectrum at the same photon energy. MBO (Aldrich Chemical Co., Inc.), purified by repeated sublimation cycles before use, was introduced into the ionization region by vaporizing the solid sample under vacuum. The temperature of the MBO during the measurements was kept constant at 110 °C. To prevent contamination of the analyzer, its lenses were heated and the interaction region was surrounded by a shield cooled with liquid nitrogen.

The ground-state equilibrium geometry and the total energy of the neutral MBO tautomers, the thione (NH) and the thiol (SH) forms (see Figure 1), have been computed by ab initio full-electron calculation at the MP2 level (Møller−Plesset second-order perturbation theory) with a 6-31G* basis set using the Gaussian 94 program.[15] The SCF eigenvectors and eigenvalues have been also obtained for both molecules at the equilibrium geometry.

The Levenburg−Marquardt nonlinear minimization algorithm with nonapproximated Voigt functions was used in the fit of both valence and C 1s PE spectra.

Results and Discussion

A. Photoelectron (PE) Spectra. *1. Valence PE Spectrum.* The experimental valence PE spectrum of MBO vapor recorded at 21.8 and 35.0 eV photon energy is reported in Figure 2. The energy scale was calibrated against the argon $3p_{3/2}$ ionization line at 15.759 eV.[16] The spectrum is characterized by a first group of four resolved photoelectron bands at 8.13 (highest occupied molecular orbital, HOMO), 8.48, 9.51, and 10.14 eV ionization potential (IP). This group is separated by a 2 eV gap from a group of unresolved bands which starts with a shoulder at 12.0 eV and extends for about 3 eV with broad peaks centered at 12.6, 13.2, 14.1, and 15.5 eV IP. It should be noted that the relative intensity of the photoionization cross section of the second ionic state at 8.48 eV strongly decreases on going from 21.8 to 35.0 eV photon energy.

Since the experimental C 1s and S 2p PE spectra are consistent with the presence of only one tautomer in the vapor phase (see below) and vibrational structure is clearly observed for the first valence PE bands, therefore we have investigated in more detail the first group of peaks. Higher resolution (60 meV) PE spectra recorded at 21.8 and 35.0 eV photon energies are shown in Figure 3 together with the result of the fit. As suggested by the observed band shape, in the analysis of the valence PE spectra, the structure of each PE band has been considered as single vibrational progression. Various fits of the experimental data have been tested. The best results have been obtained using the following procedure. For each valence PE spectrum, four sum functions have been used to fit the four peaks. To account for the vibrational progression in the photoelectron bands, the HOMO peak has been described using a sum of two Voigt components, whereas four components have been used for the second state and five for the third and fourth bands. The Voigt width parameters (Gaussian and Lorentzian) and the energy separations between the Voigt components (vibrational separation) were used as unconstrained fitting parameters. The Voigt width parameters were assumed equal for all components of each sum function. The amplitudes of each Voigt peak and the ionization potential of the first peak

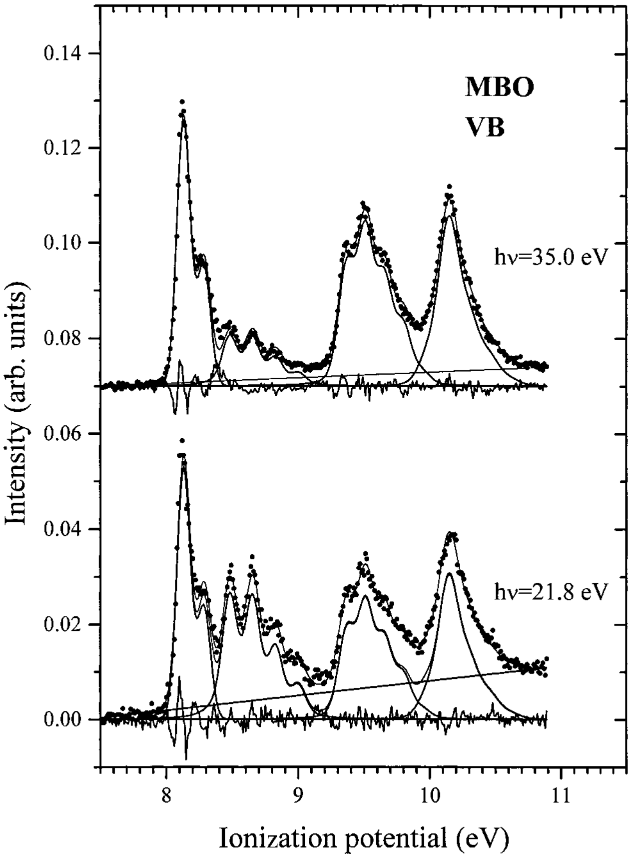

Figure 3. Outer-valence PE spectrum of MBO vapor obtained at 21.8 and 35.0 eV photon energy. The experimental curves (points) are shown together with the best fit (see text for details). The residual between the experimental data and the fit is shown below each spectrum.

TABLE 1: MBO Valence Photoemission Ionization Potential (IP)[a]

MO (NH)	$-\epsilon_{MO}$ (eV) (NH)	MO (SH)	$-\epsilon_{MO}$ (eV) (SH)	exptl IP (eV)	exptl relative intensity
7a″	8.26	7a″	8.35	8.13 (v)	100
				8.28	44
32a′	9.25	6a″	9.20	8.48 (v)	100
				8.65	95
				8.83	54
				9.00	24
					76
				9.36 (a)	
6a″	9.75	5a″	11.07	9.51 (v)	100
				9.65	66
				9.80	37
				9.94	7
					17
				9.99 (a)	
5a″	10.50	32a′	12.61	10.14 (v)	100
				10.30	38
				10.45	16
				10.60	4
4a″	13.93	4a″	13.17	12.0	
31a′	14.38	3a″	13.75	12.6	
30a′	14.63	31a′	14.07	13.2	
3a″	14.78	30a′	14.19	14.1	
29a′	15.03	29a′	14.52	15.5	
28a′	16.40	28a′	15.97		

[a] Theoretical IP values (in eV) obtained by MP2/6-31G* for vertical transitions ($-\epsilon_{MO}$) with the number and symmetry of the corresponding molecular orbital (MO) are reported for NH and SH tautomers. Experimental IP values (in eV) and corresponding relative intensities (see Figures 2 and 3) are reported (v and a in brackets mean vertical and adiabatic, respectively).

of the sum function were left free to change. For the two valence spectra recorded at different photon energies (fitted simultaneously), only the total amplitude of each of the four sum functions was allowed to change. Some fits have also been performed including the vibrational anharmonicity in the progression of the second band, but only negligible energy differences (about 5 meV) have been observed. The experimental IP values and the relative intensities of the resolved vibrational components for the first four bands are given in Table 1.

Our experimental results show that for each photoelectron band one of the possible vibrational modes of the cation is excited with higher probability. It should be noted that the appearance of vibrational progressions in PE bands for molecules of large dimensions such as MBO is rather unusual. Also in the calculated IR spectrum of the neutral MBO molecule (thione form), one vibrational mode (at 1465 cm^{-1}) strongly dominates the intensity distribution pattern.[17] The vibrational energy separations obtained by the fit of the PE spectrum are 0.153 eV (1234 cm^{-1}) for the first band (HOMO), 0.174 eV (1403 cm^{-1}) for the second band, 0.145 eV (1169 cm^{-1}) for the third band, and 0.155 eV (1250 cm^{-1}) for the fourth band. In the calculated IR spectrum, all the absorption bands in the range 1200−1500 cm^{-1} are due to vibrational modes in the molecular plane (A′ symmetry) involving the whole molecule. Because of the large number of delocalized vibrational modes it does not seem possible to give even a tentative assignment for the vibrational progression of the first four PE bands using the simple approach of comparing the molecular orbital character with the nature of calculated vibrational modes in the neutral molecule with frequencies close to the vibrational energy separations observed in the PE spectrum.

The calculated vertical ionization potentials ($-\epsilon_{MO}$) for the outermost occupied molecular orbitals (MOs) of both MBO tautomers are reported in Table 1 and Figure 2 (crosses). These values, according to the Koopmans' theorem[18] and its use in the case of the ionization of closed shell systems,[19] are derived as the negatives of the MO eigenvalues of the HF−SCF eigenvectors obtained for the neutral molecule at the equilibrium geometry.

By comparison of the experimental PE spectrum of MBO vapor with the theoretical IP values of the two tautomers, it can be observed that the calculated values for the thione form (NH) agree well with the experimental spectrum. The first group of four calculated IP values are distributed within a 2.2 eV energy range. This group is separated by a large gap from the other six IP values at higher energies. Moreover, the second occupied MO of the thione form (32 a′ in Table 1) has a large contribution of the S 3p atomic orbitals (AOs) (43.7%). This contribution is considerably larger than the one in the HOMO (7 a″) (17.4%). In the case of the thiol form (SH), the second MO (6 a″) has a negligible participation of the S 3p AOs (0.03%) while the S3p AOs contribution in the HOMO (7 a″) is 7.4%. The photoionization cross section of the S 3p AO is known to have a Cooper minimum[20] at about 35 eV, and it decreases from 4.37 to 0.52 Mb on going from 21.2 to 35.0 eV photon energy.[21] All other valence AO cross sections (C 2s, C 2p, O 2s, O 2p, N 2s, and N 2p) decrease monotonically more slowly as the photon energy increases. Therefore, the observed strong decrease in relative intensity of the second PE band at 8.48 eV IP is consistent with the presence of the thione tautomer

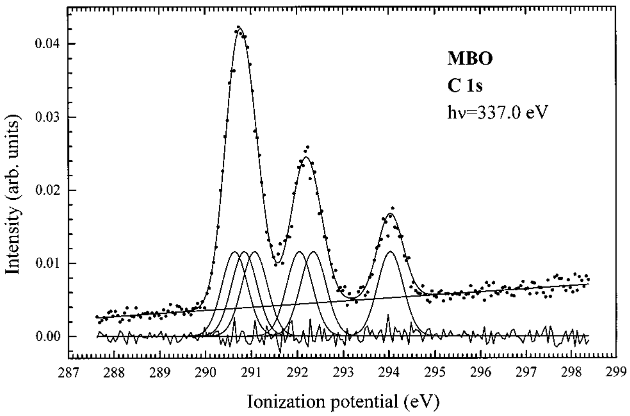

Figure 4. Carbon 1s PE spectrum of MBO vapor obtained at 337.0 eV photon energy. The experimental spectrum (points) is shown together with the best fit obtained using seven Voigt functions (see text for details). The residual between the experimental data and the fit is also reported. It should be noted that two of the Voigt functions obtained by the fit share the same ionization potential (290.64 eV).

TABLE 2: MBO C 1s Experimental and Theoretical (calculated for the thione form by ΔSCF[22] and MP2/6-31G*) Ionization Potentials (IP) Are Reported in eV[a].

	experimental IP (fit result) (eV)	theoretical IP (ΔSCF) (eV)	theoretical IP (HF MP2/6-31G*) (eV)
C_1	292.34 (1.71)	293.19 (1.77)	308.15 (1.73)
C_2	291.07 (0.43)	291.67 (0.25)	306.63 (0.21)
C_3	290.64 (0)	291.42 (0)	306.42 (0)
C_4	290.64 (0)	291.42 (0)	306.50 (0.08)
C_5	290.85 (0.21)	291.45 (0.03)	306.72 (0.30)
C_6	292.05 (1.41)	293.01 (1.59)	307.84 (1.42)
C_7	294.03 (3.39)	295.71 (4.29)	310.73 (4.31)

[a] The energy relative to the lowest value is shown in parenthesis. For the numbering of the seven carbon atoms see Figure 1

in the vapor phase. It is rather difficult, instead, to correlate the IP values calculated for the thiol form with the experimental spectrum. In addition, the calculated MP2 energy of the thione ground-state neutral molecule is lower than the one obtained for the thiol form of 1.32 Hartree.

2. C 1s and S 2p Core PE Spectra. The experimental C 1s PE spectrum of MBO and the best fit of the data are reported in Figure 4. The experimental spectrum displays three peaks with relative intensities 4:2:1. The three bands are assigned to the ionization of the seven chemically different carbon atoms of the molecule. Therefore the three peaks have been fitted using seven Voigt functions. In the fit the seven ionization potentials, amplitude, and the widths of the Voigt function were treated as free parameters (the widths and the amplitude were assumed equal for all components). It should be noted that two of Voigt functions obtained by the fit share the same ionization potential (290.64 eV).

Good agreement has been obtained between the experimental data and the sum of the seven Voigt functions. This result is in agreement with the presence of only one tautomeric form of the MBO in the vapor phase. The ionization energies of the seven components are reported in Table 2 and compared with the values obtained at ΔSCF level in ref 22 and by HF−SCF 6-31G* calculations for the thione form. The ΔSCF provides accurate absolute IP values (0.6−0.3% error) and a reliable IP distribution pattern. So, a firm assignment of the spectral features is given in the Table 2. The first peak at 294.03 eV is due to the ionization of the C_7 carbon atom that is bonded to the more electronegative atoms, namely the oxygen, sulfur, and nitrogen atoms. The second peak is ascribed to the ionization of C_1 (292.34 eV) and C_6 (292.05 eV) which are bonded to the oxygen and nitrogen atoms, respectively. The third peak, the most intense one, is assigned to the ionization of the four carbon atoms that are farthest from the electronegative heteroatoms (N and O). The two components found in the spectrum at 290.64 eV have an ionization energy close to that found for the carbon atoms in benzene (290.42 eV[23]) and can be attributed, in agreement with both calculations, to the ionization of the C_4 and C_3 atoms. The remaining two components at 290.85 and 291.07 eV are associated, according to the ΔSCF calculation, with the ionization of C_5 and C_2 atoms, respectively.

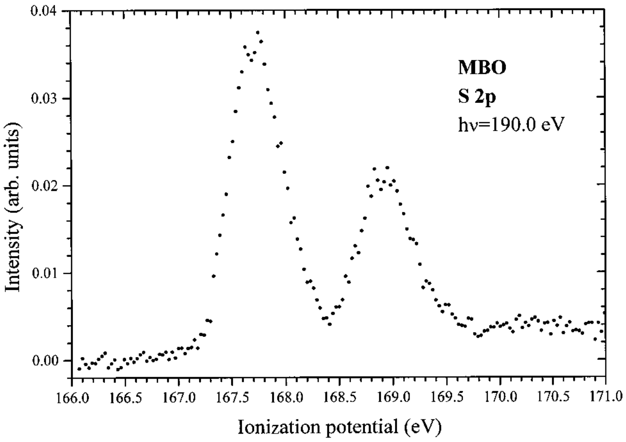

Figure 5. Sulfur 2p PE spectrum of MBO vapor obtained at 190.0 eV photon energy.

As expected, the absolute IP values obtained by the HF−SCF 6-31G* calculation on the ground state of the neutral molecule are systematically overestimated because the approach is based on the Koopmans' theorem approximation. Relaxation due to the core ionization indeed plays an important role. Nevertheless, in this simple approach the IP differences between the carbon components compare well with the experimental data and the ΔSCF calculations, with the only exception of the reverse order for the C_2 and C_5 carbon atom IP values.

The experimental S 2p PE spectrum of MBO is reported in Figure 5. Two peaks are seen at 167.7 and 168.9 eV. The intensity ratio (1.88) and the energy separation (1.2 eV), suggest an assignment of the experimental features to the two spin−orbit components $2p_{3/2}$ and $2p_{1/2}$ of the S $2p^{-1}$ core-ionized states. No other peaks are detected in this energy range. This is consistent with the existence of only one tautomeric form in the MBO vapor phase. The experimental IP value for the $2p_{1/2}$ state, 168.9 eV, can be compared with the corresponding value measured for other sulfur-containing free molecules: 171.0 eV in CS_2,[24] 171.92 eV in OCS,[25] 171.564 eV in H_2S,[26] 175.983 eV in SO_2,[27] and 181.48 eV in SF_6.[14] The large chemical shift of the S 2p ionizations in MBO is remarkable, and indicates a high electron density at the sulfur atom. The IP values measured for the MBO free molecule can be compared with the theoretical results obtained by the ΔSCF procedure in ref 22 for the thione form. The experimental and the computed IP values for the $2p_{1/2}$ state, for instance, agree within a 0.2% error (IP theoretical = 169.21 eV). The calculated IP values are therefore highly accurate.

The peak shape seen in the spectrum is asymmetric with a 0.59 eV full width at half-maximum (fwhm) for both components. The observed width is much larger than the total instrumental broadening which is estimated to be less than 240 meV. The intrinsic broadening is due to various factors, namely, the core-hole lifetime, the vibrational excitations, and the

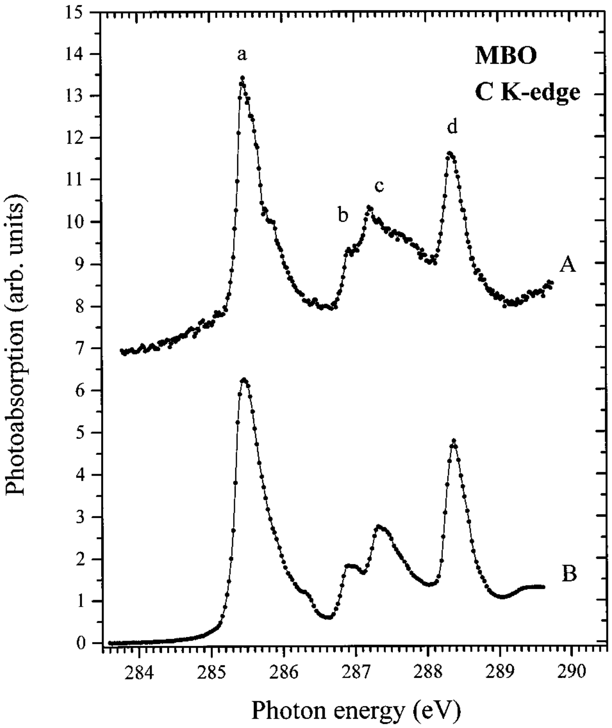

Figure 6. Total-ion-yield spectrum of MBO vapor (curve A) and experimental carbon K-edge NEXAFS spectrum of multilayer MBO on Pt(111) (curve B) from ref 22.

molecular field splitting. The splitting of the S 2p level due to the molecular field has been recently calculated as 0.15 eV at ΔSCF level, namely 168.49 and 168.34 eV IP values for the perpendicular and in the molecular plane components, respectively.[22] This value is similar to that measured in OCS.[28] The S 2p core-hole lifetime broadening calculated for the sulfur atom is 54 meV.[29] The core-hole lifetime broadening observed for highly excited Rydberg states in small molecule like SF_6,[14] H_2S,[26] and SO_2,[27] is in the 25−80 meV range, depending on the chemical environment. In MBO, however, the core-hole broadening is expected to be larger because of the high electron density at the sulfur atom that increases the Auger decay rate and shortens the core-hole lifetime. The strong asymmetry in the peak shape, as observed in small molecules,[14,27] is due to unresolved vibrational progressions in the photoelectron band. This indicates that the molecular geometry changes significantly upon ionization of the S 2p electron, and that probably the vibrational excitation gives the largest contribution to the line broadening.

B. Total-Ion-Yield Spectra (NEXAFS). *1. Carbon K-Edge*. The total ion yield spectra at the C K-edge in the 284−290 eV energy region is reported in Figure 6, curve A, together with the experimental spectrum of MBO multilayer on Pt (111), curve B, from ref 22.

The experimental features of the multilayer spectrum have been assigned on the basis of the ab initio static exchange (STEX) calculations[22] of the free molecule, performed considering only vertical transitions. The feature at 285.5 eV (transition a) has been attributed to the excitation of the π^* resonances of C_2, C_3, C_4, and C_5 atoms, the peaks at 286.9 eV (transition b), 287.4 eV (transition c), and 288.4 eV (transition d) to the excitation of the π^* resonances of C_6, C_1, and C_7, respectively. Some differences between the experimental and theoretical results can be attributed to vibrational contributions.

The experimental gas-phase spectrum (curve A) shows the same main features of the multilayer spectrum. The principal differences are observed in transitions b and c, while transitions a and d appear only lightly modified on the structures. We attribute these differences to different vibrational contributions for the two samples (multilayer and gas-phase) due to the intermolecular interactions that are present in the multilayer case.

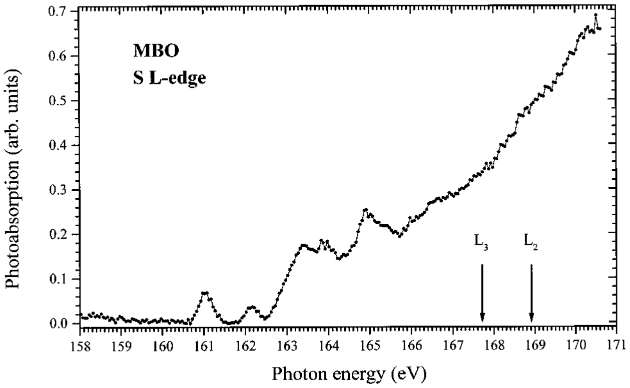

Figure 7. Total-ion-yield spectrum of MBO vapor near the sulfur $L_{2,3}$-edge. L_2 and L_3 IP values are included.

2. Sulfur L-Edge. The sulfur L-edge total-ion-yield spectrum is reported in Figure 7. Five peaks are observed at 161.0, 162.2, 163.4, 164.0, and 164.9 eV below the S 2p photoionization thresholds. The experimental features are expected to be affected by the spin−orbit splitting and the molecular field.

The assignment of the first strongest experimental peaks can be given on the basis of the results of the ab initio STEX calculation reported in ref 22. The bands at 161.0, 163.4, and 164.0 eV correspond to the three most intense transitions of the $2p_{3/2}$ core hole series calculated at 164.74, 167.13, and 167.54 eV, respectively. The second experimental structure at 162.2 eV is the $2p_{1/2}$ spin−orbit component of the first transition, as it is suggested by the 1.2 eV energy separation and the intensity ratio of about 2:1. It should be noted that the spectrum of the free MBO molecule displays a different energy pattern for the lowest transitions with respect to the multilayer MBO experimental spectrum.[22] In particular, in the gas-phase molecule the spin−orbit doublet of the lowest transition is clearly visible, while in the multilayer MBO is partially overlapping with the next transition. This difference can be ascribed to intermolecular interaction in the solid state that modify the energy levels of the empty MOs involved in the transitions.

Conclusions

In the present work the valence electronic structure of MBO vapor was investigated for the first time. The experimental PE spectrum was found in very good qualitative agreement with the MO's energies calculated at ab initio HF−SCF 6-31G* level for the thione tautomer. Assignment for the outermost valence PE bands was given on the basis of the results of the calculations. The predicted large contribution of the sulfur 3p AO to the second occupied MO (32 a′) is in accordance with the strong relative decrease of the experimental photoionization cross section of the second ionic state observed on going from 21.8 eV to the S 3p Cooper minimum photon energy (35.0 eV). The vibrational structure clearly observed for the lowest three electronic states was characterized in terms of a single progression. Adiabatic and vertical IP values were given for the lowest cation states.

The gas-phase carbon 1s and sulfur 2p PE spectra of MBO were recorded. The experimental IP values of the seven chemically different carbon atoms have been obtained and found in good agreement with the results of ab initio ΔSCF calculations for the thione form. Information on the chemical shift of the sulfur and the carbon atoms was obtained. An unusually high electron density at the sulfur atom and a low electron density at the carbon atom bound to the sulfur were found.

High-resolution total-ion-yield spectra have been recorded in the gas phase near the carbon K-edge and the sulfur $L_{2,3}$-edges. The two spectra were compared with the corresponding theoretical NEXAFS spectra calculated by the ab initio STEX method and with the experimental NEXAFS spectra of the multilayer MBO on Pt(111). In the C K-edge, some differences between the free molecule and the multilayer MBO have been observed and attributed to different vibrational contributions. Near the sulfur $L_{2,3}$-edges, a remarkable difference between the gas phase and the multilayer MBO was seen for the lowest excitations. This was attributed to the perturbation of the empty MO energies due to the intermolecular interactions in the solid state.

Acknowledgment. Two of the authors (G.C. and V.D.C.) acknowledge the financial support by “Istituto Nazionale di Fisica della Materia, I.N.F.M.” for the measurements at the ELETTRA laboratory. One of the authors (G.C.) acknowledges financial support by “CINECA” (Bologna, Italy) for the calculations. The authors thank the ELETTRA staff.

References and Notes

(1) Fang, B. S.; Olson, C. G.; Lynch, D. W. *Surf. Sci.* **1986,** *176*, 476.
(2) Wiegand, B. C.; Friend, C. M. *Chem. Rev.* **1992**, *92*, 491.
(3) Xu, Z.; Lau, S.; Bohn, P. W. *Surf. Sci.* **1993**, *296*, 57.
(4) Jaffey, D. M.; Madix, R. J. *J. Am Chem. Soc*. **1994**, *116*, 3020.
(5) Cho, K.; Kishimoto, J.; Hashizume, T.; Pickering, H. W.; Sakurai, T. *Appl. Surf. Sci*. **1995**, *87*, 380.
(6) Walsh, J. F.; Dhariwal, H. S.; Gutierrez-Sosa, A.; Finetti, P.; Muryn, C. A.; Brookes, N. B.; Oldman, R. J.; Thorton, G. *Surf. Sci*. **1998**, *415*, 423.
(7) Whelan, C. M.; Smyth, M. R.; Barnes, C. J.; Brown, N. M. D.; Aderson, C. A. *App. Surf. Sci.* **1998**, *134*, 144.
(8) Contini, G.; Ciccioli, A.; Laffon, C.; Parent, Ph.; Polzonetti, G. *Surf. Sci*. **1998**, *412/413*, 158.
(9) Contini, G.; Carravetta, V.; Parent, Ph.; Laffon, C.; Polzonetti, G. *Surf. Sci*. **2000**, *457*, 109.
(10) Marabini, A. M.; Bornego, G.; Alesse, V.; Bergamini, F. Int. Patent PCT/IT92/00148, 1992.
(11) Blyth, R. R.; Delaunay, R.; Zitnik, M.; Krempasky, J.; Krempaska, R.; Slezak, J.; Prince, K. C.; Richter, R.; Vondracek, M.; Camilloni, R.; Avaldi, L.; Coreno, M.; Stefani, G.; Furlani, C.; de Simone, M.; Stranges, S.; Adam, M. Y. *J. Electron Spectrosc. Relat. Phenom*. **1999**, *101−103*, 959.
(12) Sodhi, R. N. S.; Brion, C. E. *J. Electron Spectrosc. Relat. Phenom.* **1984**, *34*, 363.
(13) Domke, M.; Mandel, T.; Puschmann, A.; Xue, C.; Shirley, D. A.; Kaindl, G.; Petersen H.; Kuske, P. *Rev. Sci. Instrum*. **1992**, *63*, 80.
(14) Hudson, E.; Shirley, V.; Domke, M.; Remmers, G.; Puschmann, A.; Mandel, T.; Xue, C. *Phys. Rev. A* **1993**, *47*, 361.
(15) Frisch, M. J.; Trucks, G. W.; Schlegel, H. B.; Gill, P. M. W.; Johnson, B. G.; Robb, M. A.; Cheeseman, J. R.; Keith, V.; Petersson, G. A.; Montgomery, J. A.; Raghavachari, K.; Al-Laham, M. A.; Zakrzewski, V. G.; Ortiz, J. V.; Foresman, J. B.; Cioslowski, J.; Stefanov, B. B.; Nanayakkara, A.; Challacombe, M.; Peng, C. Y.; Ayala, P. Y.; Chen, W.; Wong, M. W.; Andres, J. L.; Replogle, E. S.; Gomperts, R.; Martin, R. L.; Fox, D. J.; Binkley, J. S.; Defrees, D. J.; Baker, J.; Stewart, J. P.; Head-Gordon, M.; Gonzalez, C.; Pople, J. A. *Gaussian 94, Revision C.3*; Gaussian, Inc.: Pittsburgh, PA, 1995.
(16) Lloyd, D. R. *J. Phys. E, Scient. Instrum*. **1970**, *3*, 629.
(17) Contini, G. To be published.
(18) Koopmans, T. A. *Physica* **1933**, *1*, 104.
(19) Richards, W. G. *Int. J. Mass Spectrom. Ion Phys. (Proc.)* **1969**, *2*, 419.
(20) Cooper, J. W. *Phys. Rev*. **1962**, *128*, 681.
(21) Yeh, J. J. *Atomic calculation of photoionisation cross-sections and asymmetry parameters;* Gordon and Breach Science Publisher: Langhorne, PA, 1993.
(22) Carravetta, V.; Contini, G.; Plashkevych, O.; Ågren, H.; Polzonetti, G. *J. Chem. Phys. A* **1999**, *103*, 4641.
(23) Thomas, T. D.; Shaw, R. W. *J. Electron Spectrosc. Relat. Phenom.* **1974**, *5*, 1081.
(24) Siegbahn, K.; Nordling, C.; Johansson, G.; Hedman, J.; Heden, P. F.; Hamrin, K.; Gelius, U.; Bergmark, T.; Wermer, L. O.; Manne, R.; Bear, Y. *Esca Applied to Free Molecules*, 2nd ed.; North-Holland Publishing Company: Amsterdam, 1971.
(25) Brems, V.; Nestmann, B. M.; Peyerimhoff, S. D. *Chem. Phys. Lett.* **1998**, *287*, 255.
(26) Hudson, E.; Shirley, D. A.; Domke, M.; Remmers, G.; Kaindl, G. *Phys. Rev. A* **1994**, *49*, 161.
(27) Gedat, E.; Puttner, R.; Domke, M.; Kaindl, G. *J. Chem. Phys*. **1998**, *109*, 4471.
(28) Siggel, M. R. F.; Field, C.; Saethre, L. J.; Borve, K. J.; Thomas, T. D. *J. Chem. Phys*. **1996**, *105*, 9035.
(29) Krause, M. O.; Oliver, J. H. *J. Phys. Chem. Ref. Data* **1979**, *8*, 329.